ELEKTRİK, VOL.3, NO.1, 12.1997, ©TÜBİTAK EMO

Multi-Channel Blind Image Restoration

Hung-Ta Pai, Alan C. Bovik, and Brian L. Evans
The University of Texas at Austin
Laboratory for Vision Systems
Department of Electrical and Computer Engineering
Austin, Texas 78712-1084 USA *†

Abstract

Images may be degraded for many reasons. For example, out-of-focus optics produce blurred images, and variations in electronic imaging components introduce noise. Reducing blur and noise in images is known as image restoration. In this paper, we first highlight methods for image restoration and then discuss methods for image restoration given multiple degraded copies (multiple channels) of the same original image. We focus on the blind case in which the blurring functions are unknown. We review several recently proposed algorithms for multichannel blind image restoration and present a new technique based on subspace decomposition.

1. Introduction

In many applications such as medical imaging, radio astronomy, and remote sensing, observed images are often degraded by distortion. Distortion may arise from, for example, atmospheric turbulence, relative motion between an object and the camera, and an out-of-focus camera. Restoration of the degraded images is generally required for further processing or interpretation of the images. Because constraints on the degradation and on the original image vary with the application, many different algorithms exist to solve this problem.

In some cases, the original image, which is modeled as either a deterministic or stochastic signal, is blurred by a known function. Many different conventional approaches have been developed to compensate for blur functions when they are known [1, 2]. More commonly, however, the blur function is not known. In this case, a model of the blur is often assumed, for example, a linear space-invariant filter. This kind of problem is called *blind image restoration*. A review article [3] and an updated version [4] for completeness on this topic are available. Sometimes the blur function is only partially determined, as in [5].

In some applications, several blurred versions of the same original image come from different blurring channels, or several blurred images are available from different but highly-correlated original images and channels, as in short-exposure image sequences, multispectral images, and microwave radiometric images.

* This work was sponsored in part by the US National Science Foundation CAREER Award under Grant MIP-9702707 and the US Army Research Office under Contract DAAH-04-95-I-0494.

† The authors can be reached at +1-512-471-2887 (Voice) and +1-512-471-5907 (Fax), as well as pai@vision.ece.utexas.edu, bovik@ece.utexas.edu, and bevans@ece.utexas.edu.

Restoring the original image in this situation is called *multichannel (or multiframe) blind image restoration.* Those approaches that are extensions of single-channel blind image restoration algorithms [6–8] converge to local minima, have stability problems, and require the same computational complexity, as their single-channel counterparts do [3,4]. Generally, the quality of the restored image in the multichannel case is better than in the single-channel case.

Another general class of algorithms [9,10] is an extension of blind one-dimensional (1-D) multichannel signal estimation algorithms [11,12]. Either the unknown original image or the set of blur functions is treated as deterministic so that there are no convergence or stability problems. Also, the constraints on the original image and the blur functions are very loose, but the computational complexity is relatively high.

The rest of paper focuses on multichannel blind image restoration for digital images. Section 2. describes the multichannel imaging model used throughout the paper. Section 3. reviews several approaches for multichannel blind image restoration. Section 4. corrects, discusses and analyzes a new algorithm we proposed in [9]. Finally, Section 5. concludes with a description of future work on this topic.

2. Problem Statement

Because most of the work in the image processing area is performed using computers, we will focus on digital image restoration. In general, a blurred image $x(n_1, n_2)$ can be modeled as [1]

$$x(n_1, n_2) = T\left(\sum_{l_1}\sum_{l_2} h(n_1, n_2, l_1, l_2)s(n_1, n_2)\right) \odot v(n_1, n_2) \tag{1}$$

where $\odot$ is a pointwise operation, $s(n_1, n_2)$ is the original image, $h(n_1, n_2, l_1, l_2)$ is the 2-D impulse response of the blurred system at (l_1, l_2), $v(n_1, n_2)$ is the noise, and $T(\cdot)$ generally denotes a pointwise (memoryless) operation. In remote sensing, astronomical imaging, and other image acquisition systems, the function $T(\cdot)$ models the response of an image sensor and may be nonlinear [13].

In [14] and [15], the nonlinearity of $T(\cdot)$ is considered in the restoration process. Algorithms that handle non-additive, signal-dependent noise can be found in [16] and [17]. In [18], an algorithm was developed for removing the effect of space-varying blur functions. Nevertheless, in many practical situations, and perhaps in most of the work in the image restoration area, a blurred image is modeled as the convolution of the original image and the linear space-invariant blur function plus additive and signal-independent noise.

We will now make the assumption that all blur functions are linear and space-invariant with finite support and that the noise is additive. In nearly every case in the literature, with [8] being a notable exception, the multichannel blind image restoration problem is posed as the recovery of an original image from several different blurred views of the same scene, as shown in Figure 1. The mth observed image is given by

$$x_m = h_m * s + v_m \tag{2}$$

where $*$ denotes the two-dimensional (2-D) linear convolution operator, v_m is a noise process, and x_m is the output from the mth linear space-invariant blur function h_m. The extent of the original image s is $N_1 \times N_2$ and s is indexed from $(0,0)$ to $(N_1 - 1, N_2 - 1)$. The extent of the mth blur function h_m is $L_1 \times L_2$ and h_m is indexed from $(0,0)$ to $(L_1 - 1, L_2 - 1)$. There are M observed images. Therefore, $m = 1, 2, \ldots, M$. Moreover, without any assumption about the value of the original image outside its extent, the extent of each blurred image is $(N_1 - L_1 + 1) \times (N_2 - L_2 + 1)$, i.e., from $x_m(L_1 - 1, L_2 - 1)$ to $x_m(N_1 - 1, N_2 - 1)$.

In [8], an algorithm was designed to restore multiple original images from an equal number of observed blurred images, where the blur functions *and* the original images are different but are highly correlated. Each

blurred image can be modeled as an original image convolved with a blur function with added noise. Of course, this algorithm can be applied to the situation modeled in Figure 1 by setting all of the original images to be the same, which would make the correlation among them is equal to 1, while at the same time allowing the blur functions to be different.

3. Review of Existing Algorithms

In this section, we will review four algorithms for restoring multichannel blurred images. The first three algorithms are based on single-channel blind image restoration algorithms. The fourth algorithm and our algorithm described in Section 4. are extensions of multichannel blind 1-D signal estimation algorithms.

In the area of single-channel blind image restoration, two classes of techniques are very popular and well-developed. One class utilizes stochastic models for the original image, the blur function, or the noise. The unknown model parameters are estimated from the blurred image using different approaches such as the Expectation-Maximization algorithm [19] and Generalized Cross-Validation [20]. The restored image can be obtained from these parameters. Section 3.1. discusses two recent algorithms for multichannel blind image restoration that are extensions of this kind of technique.

Instead of assuming stochastic models, the other class places deterministic constraints such as non-negativity and finite support on the original image and/or the blur function. The original image and the blur function are estimated iteratively and simultaneously. In Section 3.2., we will review a flexible framework based on this technique for the multichannel case that adds a new constraint to improve the quality of the restored image.

Recent algebraic approaches for 1-D multichannel blind signal estimation in digital communications deliver excellent performance [11, 12, 21]. They have subsequently provided another research direction in multichannel blind image restoration. Preliminary results for the 2-D case [9, 10] are based on these approaches. Section 3.3. discusses the algorithm by Giannakis and Heath [10]. In Section 4., we discuss and correct our recent result given in [9].

3.1. Maximum Likelihood (ML) Restoration Using Expectation-Maximization

We describe algorithms by Schulz [6] and Tom, Lay, and Katsaggelos [8] in this section. Their algorithms utilize stochastic models with a set of unknown parameters θ for the images, the blur functions, or the noise. Based on the stochastic model, the probability distribution function (PDF) $f_{X^M}([x_1, x_2, \ldots, x_M]|\theta)$ of the M blurred images set X^M can be found. The primary idea in maximum likelihood (ML) restoration is that θ has to be determined such that the probability of obtaining the observed blurred images $[x_1, x_2, \ldots, x_M] \in X^M$ is maximized. That is, θ has to maximize a likelihood function

$$l_{X^M}([x_1, x_2, \ldots, x_M]; \theta) = f_{X^M}([x_1, x_2, \ldots, x_M]|\theta)$$

From θ, the restored image can be obtained. In many applications, because the likelihood function includes an exponential term, it is more convenient for calculation to use a log likelihood function

$$L_{X^M}(\theta) = \log l_{X^M}([x_1, x_2, \ldots, x_M]; \theta)$$

instead of

$$l_{X^M}([x_1, x_2, \ldots, x_M]; \theta)$$

Since the logarithm is monotonically increasing, maximizing the log likelihood function is equivalent to maximizing the likelihood function.

In most situations, because the log likelihood function is very complicated, it is almost impossible to estimate the unknown parameters directly. A very powerful and popular technique, the Expectation-Maximization (EM) algorithm [19], was developed to solve this kind of problem. A tutorial article about the EM algorithm is available in [22].

In applying the EM algorithm to estimate the unknown model parameters, we define a *complete data set* $\mathbf{Z}$ such that

$$[x_1, x_2, \ldots, x_M] = g(\mathbf{z}), \text{ for some } \mathbf{z} \in \mathbf{Z}$$

where $g(\cdot)$ denotes a noninvertible many-to-one function. Note that X^M is called a *incomplete data set* in the terminology of the EM algorithm. A new log likelihood function $L_{\mathbf{Z}}(\theta)$ can be obtained from the definition of $\mathbf{Z}$.

The EM algorithm is an iterative algorithm. It includes two steps: the expectation step (E step) and the maximization step (M step). In the E step, by computing conditional probabilities for the obtained blurred images and the current estimated parameters, the expectation of $L_{\mathbf{Z}}(\theta)$ is computed. In the M step, new parameters that maximize the expectation are estimated, which become the current estimated parameters in the next iteration. Note that by choosing an adequate $g(\cdot)$ and $\mathbf{Z}$, the maximization problem will be much easier than direct maximization of $L_{X^M}([x_1, x_2, \ldots, x_M]; \theta)$. The EM algorithm can be summarized as follows:

$$\text{initial guess of } \theta_0 \rightarrow \text{E step} \rightarrow \text{M step} \rightarrow \theta_1 \rightarrow \cdots$$

The iteration continues until either a predefined number of iterations is reached or some convergence criterion is met.

Schulz [6] assumes that the blur functions and the blurred images are deterministic. Using a Poisson model for the additive noise, the log likelihood function is

$$L_{\mathbf{Z}}(\theta) = \sum_{m=1}^{M} \sum_{n_1,n_2} \sum_{l_1,l_2} [-h_m(l_1 - n_1, l_2 - n_2)s(n_1, n_2) + \tilde{x}_m(n_1, n_2, l_1, l_2) \ln (h_m(l_1 - n_1, l_2 - n_2)s(n_1, n_2))]$$

where $\theta = [s, h_1, h_2, \ldots, h_M]$ and $x_m(n_1, n_2) = \sum_{l_1,l_2} \tilde{x}_m(n_1, n_2, l_1, l_2)$. The $x_m(n_1, n_2)$ and $\tilde{x}_m(n_1, n_2, l_1, l_2)$ terms are also Poisson-distributed random variables and $E[\tilde{x}_m(n_1, n_2, l_1, l_2)] = h_m(l_1 - n_1, l_2 - n_2)s(n_1, n_2)$. Furthermore, $\{x_m(n_1, n_2)\}$ is the complete data set and $\{\tilde{x}_m(n_1, n_2, l_1, l_2)\}$ is the incomplete data set.

In some cases, a physically meaningless trivial solution, such as $s(n_1, n_2) = \delta(n_1, n_2)$, is obtained when the EM algorithm is applied to the log likelihood function. To ameliorate this problem, a penalized log likelihood function is proposed to avoid the trivial solution:

$$L^{\varphi}_{\mathbf{Z}}(\theta) = L_{\mathbf{Z}}(\theta) - \beta\varphi(s)$$

where the nonnegative scale factor β determines how strongly the penalty is enforced and $\varphi(s)$ is a penalty term that is large when the recovered image takes on the trivial solution that we want to avoid and small when it does not. One choice of the penalty term is

$$\varphi(s) = -\sum_{n_1,n_2} \ln [1 - s(n_1, n_2)]$$

Tom, Lay, and Katsaggelos [8] model the degradation process as

$$\mathbf{x} = \mathbf{Ds} + \mathbf{v}$$

where $\mathbf{s}$ is a vector composed of M blurred images with the following arrangement:

$$\mathbf{s} = [s_1(0,0), s_2(0,0), \ldots, s_M(0,0), s_1(0,1), \ldots, s_M(0,N_2-1), s_1(1,0), \ldots, s_M(N_1-1,N_2-1)]^T$$

Note that $s_m(n_1,n_2)$ is the mth original image, $m = 1,2,\ldots,M$. Here, $\mathbf{x}$ and $\mathbf{v}$ are defined with a similar arrangement as $\mathbf{s}$. $\mathbf{D}$ is an $MN_1N_2 \times MN_1N_2$ block circulant matrix of the form

$$\mathbf{D} = \begin{bmatrix} D(0) & D(1) & \cdots & D(N_1N_2-1) \\ D(N_1N_2-1) & D(0) & \cdots & D(N_1N_2-2) \\ \vdots & \vdots & \ddots & \vdots \\ D(1) & D(2) & \cdots & D(0) \end{bmatrix}$$

where the $M \times M$ submatrices $D(n)$ for $1 \le n \le N_1N_2$ are defined according to

$$D(n) = \begin{bmatrix} D_{11}(n) & D_{12}(n) & \cdots & D_{1M}(n) \\ D_{21}(n) & D_{22}(n) & \cdots & D_{2M}(n) \\ \vdots & \vdots & \ddots & \vdots \\ D_{M1}(n) & D_{M2}(n) & \cdots & D_{MM}(n) \end{bmatrix}$$

Note that $D_{ii}(n)$ denotes the intrachannel blur, and $D_{ij}(n), i \neq j$, denotes the interchannel blur.

Moreover, we assume that $\mathbf{s}$ and $\mathbf{v}$ are uncorrelated Gaussian random processes, and that $\mathbf{x}$ is also Gaussian with zero mean. We define $\mathbf{x} = g(\mathbf{z})$ where $\mathbf{z} = [\mathbf{s}, \mathbf{x}]$ and $\{\mathbf{z}\}$ is the complete data set and $\{\mathbf{x}\}$ is the incomplete data set to obtain a log likelihood function with $\theta = [\Lambda_X, \Lambda_V, \mathbf{D}]$, where Λ_X is the image covariance matrix and Λ_V is the noise covariance matrix. By transforming the expectation of the likelihood function to the frequency domain and using Wiener filtering, θ can be computed and $\mathbf{s}$ can be estimated.

The advantages of the previous algorithms are that they guarantee convergence and low computational complexity ($O(ML_1L_2N_1N_2)$). The disadvantage is that the EM algorithm could converge to a local optimum. Thus, the initial guess of θ is very important and several applications of the algorithm on the same blurred images may be required.

3.2. Iterative Blind Image Restoration Based on Deterministic Constraints

Miura and Baba [7] extended the *iterative blind image restoration algorithm* developed for the single-channel case by Ayers and Dainty [23], as shown in Figure 2(a), to multiple channels, as shown in Figure 2(b). In the single-channel situation, Ayers and Dainty [23] placed nonnegativity constraints on the image and the blur function, and Wiener filtering is adopted in the Fourier domain to obtain $\hat{S}_k$ and $\hat{H}_k$. Miura and Baba proposed an extra constraint that the blurred images are from the same original image. The evaluation function $Q(i)$ in the ith iteration is defined as follows:

$$Q(i) = \min_{0 \le m \le M-1} \{C[s_i^m(n_1,n_2), s_i^{m+1}(n_1,n_2)]\}$$

Here, $C[\cdot,\cdot]$ is the maximum value of the normalized cross-correlation from 0 to 1 between two functions. After I iterations, the output image, i.e., the restored image, of this algorithm is $\bar{s}_{i'}(n_1,n_2)$ where

$$i' = \arg \max_{1 \le i \le I} Q(i)$$

since the difference among the output images from the single-channel blind deconvolution blocks in each iteration should be as small as possible. The reason is that the blurred images are from the same original

image. When $Q(i')$ is larger than a threshold t_Q, $\bar{s}_{i'}$ is accepted as a restored image. Note that I and t_Q are chosen heuristically; e.g., Miura and Baba [7] choose $I = 100$ and $t_Q = 0.97$.

The primary advantage of this algorithm is flexibility. Different single-channel blind image restoration algorithms of this class [23–25] can be substituted for the single-channel blind deconvolution blocks in Figure 2(b). But this algorithm will have the same advantages, such as low computational complexity, and disadvantages, such as high sensitivity to the initial image estimate and poor convergence properties.

3.3. Two Algebraic Approaches for Image Restoration

Giannakis and Heath [10] proposed two algebraic approaches for the multichannel blind image restoration problem. These approaches extend blind 1-D channel identification algorithms developed in [12, 21, 26] for application in communication systems. The first approach is to identify the blur functions, and then, use a conventional image restoration algorithm such as the Wiener filter technique to recover the original image. The second approach is to find the $M \times 1$ vector restoration filter

$$\mathbf{g}^{i_1,i_2}(k_1,k_2) = [g_1^{i_1,i_2}(k_1,k_2), g_2^{i_1,i_2}(k_1,k_2), \ldots, g_M^{i_1,i_2}(k_1,k_2)]^T \tag{3}$$

so that, when no noise is present,

$$\sum_{k_1=1}^{K_1}\sum_{k_2=1}^{K_2} \mathbf{x}(n_1-k_1+1, n_2-k_2+1)^T \mathbf{g}^{i_1,i_2}(k_1,k_2) = s(n_1-i_1, n_2-i_2) \tag{4}$$

where (K_1, K_2) is chosen such that (4) has a solution, $0 \le i_j \le L_j + K_j - 1$ for $j = 1, 2$, and

$$\mathbf{x}(n_1,n_2) = [x_1(n_1,n_2), x_2(n_1,n_2), \ldots, x_M(n_1,n_2)]^T \tag{5}$$

In the first approach, by neglecting the noise term, we rewrite (2) as

$$\begin{aligned} x_{m_1} &= h_{m_1} * s \\ x_{m_2} &= h_{m_2} * s \end{aligned}$$

where $1 \le m_1, m_2 \le M$ and $m_1 \ne m_2$. Then,

$$\begin{aligned} h_{m_2} * x_{m_1} &= h_{m_2} * h_{m_1} * s \\ &= h_{m_1} * h_{m_2} * s \\ &= h_{m_1} * x_{m_2} \end{aligned}$$

Therefore,

$$x_{m_2} * h_{m_1} - x_{m_1} * h_{m_2} = 0 \tag{6}$$

Based on the relation in (6), we can construct a $\frac{1}{2}M(M-1)(N_1-L_1+2)(N_2-L_2+2) \times ML_1L_2$ matrix $\mathbf{X}_{L_1,L_2}$ from the blurred images x_m for $m = 1, 2, \ldots, M$, such that

$$\mathbf{X}_{L_1,L_2}\mathbf{h} = 0 \tag{7}$$

where

$$\mathbf{h} = [h_1(0,0), h_1(0,1), \ldots, h_1(L_1-1, L_2-1), h_2(0,0), \ldots, h_M(L_1-1, L_2-1)]^T$$

When the rank of $\mathbf{X}_{L_1,L_2}$ equals $ML_1L_2 - 1$, a unique solution for $\mathbf{h}$ in (7) exists because the nullspace of $\mathbf{X}_{L_1,L_2}$ has dimension 1. If additive noise is present, $\mathbf{h}$ can be obtained from the eigenvector of $\mathbf{X}_{L_1,L_2}$ corresponding to the smallest eigenvalue.

The second approach follows similar steps as (3) to (5) but with

$$\sum_{k_1=1}^{K_1}\sum_{k_2=1}^{K_2}\left[\mathbf{x}(n_1-i_1-k_1,n_2-i_2-k_2)^T \quad -\mathbf{x}(n_1-i_1'-k_1,n_2-i_2'-k_2)^T\right]\begin{bmatrix}\mathbf{g}^{i_1',i_2'}(k_1,k_2)\\ \mathbf{g}^{i_1,i_2}(k_1,k_2)\end{bmatrix}=0 \qquad (8)$$

for $K_j+i_j \le n_j \le N_j$ and $0 \le i_j' < i_j \le L_j+K_j-1$, where $j=1,2$. We can write (8) as a $1\times 2MK_1K_2$ row vector times a $2MK_1K_2\times 1$ column vector. Based on (8), we can form the matrix equation

$$\mathbf{X}\,\hat{\mathbf{g}}=0 \qquad (9)$$

where

$$\hat{\mathbf{g}}=[\mathbf{g}^{0,0}(1,1)^T,\mathbf{g}^{0,0}(1,2)^T,\ldots,\mathbf{g}^{0,0}(K_1,K_2)^T,\mathbf{g}^{0,1}(1,1)^T,\ldots,\mathbf{g}^{L_1+K_1-1,L_2+K_2-1}(K_1,K_2)^T]^T$$

and $\mathbf{X}$ is obtained by the proper rearrangement of (8). $\mathbf{X}$ is a sparse matrix with exactly $2K_1K_2$ non-zero elements in each row. $\mathbf{X}$ contains $\sum_{i_1,i_2}(N_1-K_1+1)(N_2-K_2+1)-i_1(N_2-K_2+1)-i_2$ rows and $MK_1K_2(L_1+K_1)(L_2+K_2)$ columns. If the rank of $\mathbf{X}$ equals $MK_1K_2(L_1+K_1)(L_2+K_2)-1$, then (9) has a unique solution for $\hat{\mathbf{g}}$ and the original image can be recovered exactly by (4). Giannakis and Heath [10] do not report a noisy case for the second approach.

These two algebraic approaches offer three key advantages: no initial image is required, the constraints on the original image and the blur functions are very loose, and no convergence or stability problems exist. Nevertheless,the first approach requires a conventional image restoration technique to recover the original image and the second approach amplifies noise. The computational complexity in these two approaches is relatively high because of the definition of large matrices and operations performed on them.

4. A New Algebraic Approach

Recently, we extended a blind one-dimensional multi-channel symbol estimation algorithm [11] to two dimensions [9]. We have proved sufficient conditions to achieve exact restoration of blurred images in the noise-free case;i.e., the restored image is the same as the original image up to a scalar multiplier. In this section, we make a correction to the sufficient conditions. Moreover, we provide a more advanced discussion and analysis of this algorithm.

4.1. Derivation and Correction

In the noiseless case, we construct a block Hankel matrix

$$\mathbf{X}(K_1,K_2)=\begin{bmatrix}
\mathbf{x}(L_1-1,L_2-1) & \cdots & \mathbf{x}(L_1-1,N_2-K_2) & \cdots & \mathbf{x}(N_1-K_1,N_2-K_2)\\
\mathbf{x}(L_1-1,L_2) & \cdots & \mathbf{x}(L_1-1,N_2-K_2+1) & \cdots & \mathbf{x}(N_1-K_1,N_2-K_2+1)\\
\vdots & \vdots & \vdots & \vdots & \vdots\\
\mathbf{x}(L_1-1,L_2+K_2-2) & \cdots & \mathbf{x}(L_1-1,N_2-1) & \cdots & \mathbf{x}(N_1-K_1,N_2-1)\\
\mathbf{x}(L_1,L_2-1) & \cdots & \mathbf{x}(L_1,N_2-K_2) & \cdots & \mathbf{x}(N_1-K_1+1,N_2-K_2)\\
\vdots & \vdots & \vdots & \vdots & \vdots\\
\mathbf{x}(R_1,R_2) & \cdots & \mathbf{x}(R_1,N_2-1) & \cdots & \mathbf{x}(N_1-1,N_2-1)
\end{bmatrix} \qquad (10)$$

where $R_1 = L_1 + K_1 - 2, R_2 = L_2 + K_2 - 2$, K_1 and K_2 are chosen to satisfy the exact restoration conditions, and $\mathbf{x} = [x_1, x_2, \cdots, x_M]^T$ is a vector of matrices containing the blurred images. Define

$\mathbb{C}(z)$ is the set of all rational functions in z over the complex number set $\mathbb{C}$

V is the k-dimensional vector space of n-tuples over $\mathbb{C}(z)$

$\mathbf{h} = [h_1, h_2, \ldots, h_M]^T$

$$H_l = \underbrace{\begin{bmatrix} \mathbf{h}(l, L_2-1) & \cdots & \mathbf{h}(l,1) & \mathbf{h}(l,0) & \mathbf{0} & \cdots & \mathbf{0} \\ \mathbf{0} & \mathbf{h}(l, L_2-1) & \cdots & \mathbf{h}(l,1) & \mathbf{h}(l,0) & \ddots & \vdots \\ \vdots & \ddots & \ddots & \ddots & \ddots & \ddots & \ddots \\ \mathbf{0} & \cdots & \mathbf{0} & \mathbf{h}(l, L_2-1) & \cdots & \mathbf{h}(l,1) & \mathbf{h}(l,0) \end{bmatrix}}_{R_2+1 \text{ blocks}}$$

$$\mathbf{H} = \underbrace{\begin{bmatrix} H_{L_1-1} & \cdots & H_1 & H_0 & \mathbf{0} & \cdots & \mathbf{0} \\ \mathbf{0} & H_{L_1-1} & \cdots & H_1 & H_0 & \ddots & \vdots \\ \vdots & \ddots & \ddots & \ddots & \ddots & \ddots & \ddots \\ \mathbf{0} & \cdots & \mathbf{0} & H_{L_1-1} & \cdots & H_1 & H_0 \end{bmatrix}}_{R_1+1 \text{ blocks}}$$

and

$$\mathbf{S}(R_1, R_2) = \begin{bmatrix} s(0,0) & \cdots & s(0, N_2-R_2-1) & s(1,0) & \cdots & s(N_1-R_1-1, N_2-R_2-1) \\ s(0,1) & \cdots & s(0, N_2-R_2) & s(1,1) & \cdots & s(N_1-R_1-1, N_2-R_2) \\ \vdots & \vdots & \vdots & \vdots & \vdots & \vdots \\ s(0,R_2) & \cdots & s(0, N_2-1) & s(1,R_2) & \cdots & s(N_1-R_1-1, N_2-1) \\ s(1,0) & \cdots & s(1, N_2-R_2-1) & s(2,0) & \cdots & s(N_1-R_1, N_2-R_2-1) \\ \vdots & \vdots & \vdots & \vdots & \vdots & \vdots \\ s(R_1,R_2) & \cdots & s(R_1, N_2-1) & s(R_1+1,R_2) & \cdots & s(N_1-1, N_2-1) \end{bmatrix}$$

Then

$$\mathbf{X}(K_1, K_2) = \mathbf{H}\,\mathbf{S}(R_1, R_2)$$

The following definitions are similar to those definitions in [27].

- *Definition 1*: The *degree* $\deg \mathbf{f}$ of an n-tuple $\mathbf{f} = [f_1, f_2, \ldots, f_n]^T$ of polynomials is the greatest degree of its components $f_j, 1 \le j \le n$.
- *Definition 2*: If F is a $n \times k$ polynomial matrix with columns $\mathbf{f}_i$, the ith index of F is defined as $v_i = \deg \mathbf{f}_i, 1 \le i \le k$, and the *order* of F is defined as $v = \sum_{i=1}^{k} v_i$.
- *Definition 3*: A minimal basis of V is a $n \times k$ polynomial matrix F such that F is a basis for V and F has least order among all polynomial bases for V.
- *Definition 4*: The *invariant dynamic indices* v_i of V are the indices of any minimal basis for V. Its *invariant dynamical order* v is the sum of the v_i.

- *Definition 5*: If F is a full-rank $n \times k$ matrix over $\mathbb{C}(z)$, then the set of all row n-tuples $\mathbf{x}$ such that $\mathbf{x}F = 0$ is a vector space over $\mathbb{C}(z)$, called the *dual space*.

- *Definition 6*: The *high-order coefficient matrix* $[F]_h$ of F is the $n \times k$ matrix whose ith column consists of the coefficients of x^{v_i} in the ith column $\mathbf{f}_i$ of F.

- *Lemma 1*: The invariant dynamical orders of V and its dual space U are the same. [27]

- *Lemma 2*: F is a minimal basis for a k-dimensional vector space V of n-tuples over $\mathbb{C}(z)$ if and only if [27]

  1. The greatest common divisor of all minors of F is 1.
  2. The greatest degree of all minors of F is v;i.e., the high-order coefficient matrix $[F]_h$ is of full column rank.

- *Lemma 3*: Given an $r \times r$ matrix polynomial $C(z) = \sum_{i=0}^{d} C_i z^i$ and a $q \times r$ matrix polynomial $D(z) = \sum_{i=0}^{d} D_i z^i$, we have [28]

$$\text{rank}(S) = (r+q)k - \sum_{i:u_i<k} (k - u_i)$$

  where

$$S = \underbrace{\begin{bmatrix} D_0 & D_1 & \cdots & D_d & \mathbf{0} & \cdots & \mathbf{0} \\ C_0 & C_1 & \cdots & C_d & \mathbf{0} & \cdots & \mathbf{0} \\ \mathbf{0} & D_0 & \cdots & D_{d-1} & C_d & \ddots & \vdots \\ \mathbf{0} & C_0 & \cdots & C_{d-1} & C_d & \ddots & \vdots \\ \vdots & \ddots & \ddots & \ddots & \ddots & \ddots & \ddots \\ \mathbf{0} & \cdots & \mathbf{0} & D_0 & \cdots & D_{d-1} & D_d \\ \mathbf{0} & \cdots & \mathbf{0} & C_0 & \cdots & C_{d-1} & C_d \end{bmatrix}}_{2k \text{ blocks}}$$

  is called the generalized Sylvester resultant of C and D, and the u_i terms for $i = 1, 2, \ldots, q$ are the invariant dynamic indices of $U_{r\times(q+r)}$, a.k.a. the dual dynamic indices [27] of the transfer function $D(z)C(z)^{-1}$. Let $[D(z)^T \; C(z)^T]^T$ be a basis of a r-dimensional vector space $V_{(q+r)\times r}$ of $(q+r)$-tuples over $\mathbb{C}(z)$. Note that $U_{r\times(q+r)}$ is the dual space of $V_{(q+r)\times r}$. For convenience, we call u_i for $i = 1, 2, \ldots, q$ the dual dynamic indices from $[D(z)^T \; C(z)^T]^T$.

- *Lemma 4*: H_0 can be cycloextended to be full column rank;i.e., $\text{rank}(H_0) = R_2 + 1$ by choosing $K_2 > L_2 - 1$ if

  1. $h_m(0,0)$ terms for $m = 1, 2, \ldots, M$ are not all zeros, and
  2. the polynomials $h_m(0,z) = \sum_{l_2=0}^{L_2-1} h_m(0, L_2 - l_2 - 1) z^{l_2}$, for $m = 1, 2, \ldots, M$ do not share a common zero.

  Proof: The proof is similar to the one in [29]. Define a matrix polynomial

$$\mathbf{h}_0(z) = [h_1(0,z), h_2(0,z), \ldots, h_m(0,z)]^T$$

Since conditions 1 and 2 imply the conditions 2 and 1 in *Lemma 2*, respectively, $\mathbf{h}_0(z)$ is a minimal basis for a 1-dimensional vector space of M-tuples over $\mathbb{C}(z)$. Let u_i^z for $i = 1, 2, \ldots, M-1$ be the dual dynamic indices for $\mathbf{h}_0(z)$. From *Lemma 1*, $\sum_{i=1}^{M-1} u_i^z = L_2 - 1$. From *Lemma 3*, by choosing $K_2 > L_2 - 1$,

$$\begin{aligned} \text{rank}(H_0) &= MK_2 - \sum_{i=1}^{M-1} (K_2 - u_i^z) \\ &= K_2 + L_2 - 1 \\ &= R_2 + 1 \end{aligned}$$

□

- *Lemma 5*: $\mathbf{H}$ can be cycloextended to be of full column rank;i.e., $\text{rank}(\mathbf{H}) = (R_1+1)(R_2+1)$, by choosing $K_1 > (L_1-1)(R_2+1)$ and $K_2 > L_2 - 1$ if

  1. the polynomials
  $$\sum_{l_1=0}^{L_1-1} \sum_{l_2=0}^{L_2-1} h_m(L_1 - l_1 - 1, L_2 - l_2 - 1) z_1^{l_1} z_2^{l_2}$$
  for $m = 1, 2, \ldots, M$ do not share any common zeros,
  2. $h_m(0,0)$ terms for $m = 1, 2, \ldots, M$ are not all zeros,
  3. the polynomials
  $$\sum_{l_1=0}^{L_1-1} h_m(L_1 - l_1 - 1, 0) z_1^{l_1}$$
  for $m = 1, 2, \ldots, M$, do not share any common zeros, and
  4. the polynomials
  $$\sum_{l_2=0}^{L_2-1} h_m(0, L_2 - l_2 - 1) z_2^{l_2}$$
  for $m = 1, 2, \ldots, M$ do not share any common zeros.

  Proof: See Appendix A. □

In our simulations, the above conditions are satisfied very easily when $M > 2$. Moreover, choosing $K_1 \geq 2(L_1 - 1)$ and $K_2 \geq L_2 - 1$ is enough to make $\mathbf{H}$ be of full column rank. From *Lemma 5* and [9], we find if

1. the polynomials
$$\sum_{l_1=0}^{L_1-1} \sum_{l_2=0}^{L_2-1} h_m(L_1 - l_1 - 1, L_2 - l_2 - 1) z_1^{l_1} z_2^{l_2}$$
for $m = 1, 2, \ldots, M$ do not share any common zeros,
2. $h_m(0,0)$ terms for $m = 1, 2, \ldots, M$ are not all zeros,
3. the polynomials $\sum_{l_1=0}^{L_1-1} h_m(L_1 - l_1 - 1, 0) z_1^{l_1}$ for $m = 1, 2, \ldots, M$ do not share any common zeros,
4. the polynomials $\sum_{l_2=0}^{L_2-1} h_m(0, L_2 - l_2 - 1) z_2^{l_2}$ for $m = 1, 2, \ldots, M$ do not share any common zeros, and
5. $\mathbf{S}(R_1+1, R_2)$ and $\mathbf{S}(R_1, R_2+1)$ have full row rank,

then the null space of $\mathbf{X}(K_1, K_2)$ is identical to the null space of $\mathbf{S}(R_1, R_2)$. Let $\mathbf{N}$ be the null space of $\mathbf{X}(K_1, K_2)$ and define

$$\begin{aligned}\mathbf{w}_{i,j} &= [\mathbf{N}((N_2-R_2)i+j,0), \mathbf{N}((N_2-R_2)i+j,1), \ldots \\ &\quad \mathbf{N}((N_2-R_2)i+j,(N_1-R_1)(N_2-R_2)-(R_1+1)(R_2+1)-1)]^T \\ W_i &= \underbrace{\begin{bmatrix} \mathbf{w}_{i,0} & \mathbf{w}_{i,1} & \cdots & \mathbf{w}_{i,N_2-R_2-1} & \mathbf{0} & \cdots & \mathbf{0} \\ \mathbf{0} & \mathbf{w}_{i,0} & \mathbf{w}_{i,1} & \cdots & \mathbf{w}_{i,N_2-R_2-1} & \ddots & \vdots \\ \vdots & \ddots & \ddots & \ddots & \ddots & \ddots & \ddots \\ \mathbf{0} & \cdots & \mathbf{0} & \mathbf{w}_{i,0} & \mathbf{w}_{i,1} & \cdots & \mathbf{w}_{i,N_2-R_2-1} \end{bmatrix}}_{N_2 \text{ blocks}}\end{aligned}$$

We can construct a matrix $\mathbf{W}$ from the the null space of $\mathbf{X}(K_1, K_2)$ such that

$$\mathbf{W}\tilde{\mathbf{s}} = \mathbf{0}, \tag{11}$$

where

$$\tilde{\mathbf{s}} = [s(0,0), s(0,1), \ldots, s(0,N_2-1), s(1,0), \ldots, s(N_1-1,N_2-1)]^T, \text{ and}$$

$$\mathbf{W} = \underbrace{\begin{bmatrix} W_0 & W_1 & \cdots & W_{N_1-R_1-1} & \mathbf{0} & \cdots & \mathbf{0} \\ \mathbf{0} & W_0 & W_1 & \cdots & W_{N_1-R_1-1} & \ddots & \vdots \\ \vdots & \ddots & \ddots & \ddots & \ddots & \ddots & \ddots \\ \mathbf{0} & \cdots & \mathbf{0} & W_0 & W_1 & \cdots & W_{N_1-R_1-1} \end{bmatrix}}_{N_1 \text{ blocks}}$$

We can exactly restore the image up to a scalar multiple of the unique solution of (11). Based on this derivation, we propose the following algorithm for exact multi-channel blind image restoration:

1. Construct $\mathbf{X}(K_1, K_2)$ from the blurred images according (10).
2. Find the null space $\mathbf{N}$ of $\mathbf{X}$.
3. Construct $\mathbf{W}$ from $\mathbf{N}$.
4. Solve $\mathbf{W}\tilde{\mathbf{s}} = \mathbf{0}$.

In the noisy case, it is possible to restore the image from the eigenvector of $\mathbf{W}$ corresponding to the smallest eigenvalue.

4.2. Examples

We present several simulations under different conditions using $L_1 \times L_2$ FIR blur functions, M blurred versions of the original image, and different SNR values:

1. $L_1 = L_2 = 3$, $M = 3$, and $SNR = 60$ dB.
2. $L_1 = L_2 = 3$, $M = 6$, and $SNR = 60$ dB.

3. $L_1 = L_2 = 5,\ M = 6$, and $SNR = 60$ dB.

4. $L_1 = L_2 = 3,\ M = 3$, and $SNR = 50$ dB.

5. $L_1 = L_2 = 3,\ M = 6$, and $SNR = 50$ dB.

6. $L_1 = L_2 = 5,\ M = 6$, and $SNR = 50$ dB.

We generate blur functions by generating random filter coefficients for the $L_1 \times L_2$ FIR filters. We estimate the original image directly with knowledge of L_1 and L_2 but without having to estimate the blur functions. We coded the algorithm in C using the LAPACK library. The original image is shown in Figure 3 and the deblurred results are shown in Figures 4, 5, 6, 7, 8, and 9.

4.3. Evaluation

From the examples, we conclude that

1. For the same SNR and number of blurred images, the higher the order of the blur functions, the lower the quality of the restored images, as shown in Figures 5, 6, 8, and 9.

2. For the same SNR and order of the blur functions, the greater the number of blurred images, the better the quality of the restored images, as in Figure 4, 5, 7, and 8.

3. The lower the SNR, the lower the quality of the restored images.

In item 1, we assume that we chose the filter order that is the best match to the blur functions. For higher filter orders, every pixel in the restored image is affected by more neighboring pixels. Thus, it is more difficult to recover the original image exactly. Items 2 and 3 are intuitive.

Compared with the algorithm in Section 3.3., our algorithm offers the same three advantages but restores an image from a set of blurred versions directly without relying on a conventional image restoration algorithm and without amplifying noise. Neither a restoration filter nor the identification of blur functions is required. Therefore, our algorithm will not suffer from the disadvantages of conventional image restoration algorithms or from noise amplification. Nevertheless, the computational complexity is also high.

5. Conclusions and Future Work

In this paper, we reviewed several existing techniques for multichannel blind image restoration. Some of them were based on single-channel blind image restoration algorithms. The others extended blind 1-D multichannel signal estimation algorithms. Additionally, we corrected the sufficient conditions of a new technique, analyzed its performance, and demonstrated its advantages of having no convergence or stability problems, placing no requirement on providing an initial guess of the image, and requiring only loose constraints on the original image and the blur functions. In the future, we will work on how to reduce the computation cost of this algorithm and apply it to images of satellites.

Appendix: Proof of Lemma 5

This proof is separated into three steps. First, we want to show

$$\sum_{l_1=0}^{L_1-1} H_{L_1-l_1-1} z_1^{l_1}$$

has full column rank by contradiction. Assume that there exists a_1 such that

$$S = \sum_{l_1=0}^{L_1-1} H_{L_1-l_1-1} a_1^{l_1}$$

is not of full column rank. That is, $\text{rank}(S) < R_2 + 1$. From *Lemma 3*,

$$MK_2 - \sum_{i:u_i^{z_2}<K_2} (K_2 - u_i^{z_2}) < R_2 + 1 \tag{12}$$

where $u_i^{z_2}, i = 1, 2, \ldots, M-1$ are the dual dynamic indices from

$$\sum_{l_1=0}^{L_1-1} \sum_{l_2=0}^{L_2-1} \mathbf{h}(L_1 - l_1 - 1, L_2 - l_2 - 1) a_1^{l_1} z_2^{l_2}$$

We obtain $K_2 > u_i^{z_2}$ by choosing $K_2 > L_2 - 1$ because, from *Definition 3, 4* and *Lemma 1*, $\sum_{i=1}^{M-1} u_i^{z_2}$ is less than or equal to $L_2 - 1$, i.e., the maximum order of polynomials

$$\sum_{l_1=0}^{L_1-1} \sum_{l_2=0}^{L_2-1} h_m(L_1 - l_1 - 1, L_2 - l_2 - 1) a^{l_1} z_2^{l_2}$$

Therefore, $\sum_{i=1}^{M-1} u_i^{z_2} < L_2 - 1$ from (12). Condition 3 implies $\sum_{l_1=0}^{L_1-1} h_m(L_1 - l_1 - 1, 0) a^{l_1}$ for $m = 1, 2, \ldots, M$ are not all zeros. From *Lemma 3*,

$$\sum_{l_1=0}^{L_1-1} \sum_{l_2=0}^{L_2-1} h_m(L_1 - l_1 - 1, L_2 - l_2 - 1) a^{l_1} z_2^{l_2}$$

for $m = 1, 2, \ldots, M$, share a common zero at least, say a_2. The term (a_1, a_2) is a common zero of

$$\sum_{l_1=0}^{L_1-1} \sum_{l_2=0}^{L_2-1} h_m(L_1 - l_1 - 1, L_2 - l_2 - 1) z_1^{l_1} z_2^{l_2}$$

for $m = 1, 2, \ldots, M$. This contradicts condition 1.

Second, we want to prove that all minors of $\sum_{l_1=0}^{L_1-1} H_{L_1-l_1-1} z_1^{l_1}$ have no common divisor $p(z_1)$, where $p(z_1)$ is non-trivial, by contradiction also. Let one of roots of $p(z_1)$ be a_1. Therefore, all minors of $\sum_{l_1=0}^{L_1-1} H_{L_1-l_1-1} a^{l_1}$ should be zero and $\sum_{l_1=0}^{L_1-1} H_{L_1-l_1-1} a^{l_1}$ does not have full column rank. This contradicts the result of the first step.

Finally, from *Lemma 4*, when conditions 2 and 4 hold, H_0 has full column rank. We can conclude $\sum_{l_1=0}^{L_1-1} H_{L_1-l_1-1} z_1^{l_1}$ is a minimal basis for an (R_2+1)-dimensional vector space of MK_2-tuples over $\mathbb{C}(z)$ from *Lemma 2*. Then, $\sum_{i=1}^{MK_2-R_2-1} u_i^{z_1} = (L_1 - 1)(R_2 + 1)$, where $u_i^{z_1}, i = 1, 2, \ldots, MK_2 - R_2 - 1$, are the

dual dynamic indices from $\sum_{l_1=0}^{L_1-1} H_{L_1-l_1-1} z_1^{l_1}$. We obtain $K_1 > u_i^{z_1}$ by choosing $K_1 > (L_1-1)(R_2+1)$. Therefore,

$$\begin{aligned}
\text{rank}(\mathbf{H}) &= MK_1K_2 - \sum_{i:K_1>u_i^{z_1}} (K_1 - u_i^{z_1}) \\
&= MK_1K_2 - (MK_2 - R_2 - 1)K_1 + \sum_{i=1}^{MK_2-R_2-1} u_i^{z_1} \\
&= (R_2+1)K_1 + (L_1-1)(R_2+1) \\
&= (R_1+1)(R_2+1)
\end{aligned}$$

□

References

References

[1] A. K. Katsaggelos (Ed.), *Digital Image Restoration*. Berlin: Springer-Verlag, 1991.

[2] M. R. Banham and A. K. Katsaggelos, "Digital image restoration," *IEEE Signal Processing Magazine*, vol. 14, pp. 24–41, Mar. 1997.

[3] D. Kundur and D. Hatzinakos, "Blind image deconvolution," *IEEE Signal Processing Magazine*, vol. 13, pp. 43–64, May 1996.

[4] D. Kundur and D. Hatzinakos, "Blind image deconvolution revisited," *IEEE Signal Processing Magazine*, vol. 13, pp. 61–63, Nov. 1996.

[5] R. K. Ward, "Restoration of differently blurred versions of an image with measurement errors in the PSF's," *IEEE Trans. on Image Processing*, vol. 2, pp. 369–381, July 1993.

[6] T. J. Schulz, "Multiframe blind deconvolution of astronomical images," *J. Opt. Soc. Am. A.*, vol. 10, pp. 1064–1073, May 1993.

[7] N. Miura and N. Baba, "Extended-object reconstruction with sequential use of the iterative blind deconvolution method," *Optics Communications*, vol. 89, pp. 375–379, May 1992.

[8] B. C. Tom, K. T. Lay, and A. K. Katsaggelos, "Multichannel image identification and restoration using the Expection-Maximization algorithm," *Optical Engineering*, vol. 35, pp. 241–254, Jan. 1996.

[9] H. T. Pai and A. C. Bovik, "Exact multichannel blind image restoration," *Signal Processing Letters*, vol. 4, pp. 217–220, Aug. 1997.

[10] G. B. Giannakis and R. W. Heath, Jr., "Blind identification of multichannel FIR blur and perfect image restoration," in *Proc. IEEE Int. Conf. Image Processing*, vol. 1, (Lausanne, Switzerland), pp. 717–720, Sept. 1996.

[11] H. Liu and G. Xu, "Closed-form blind symbol estimation in digital communications," *IEEE Trans. on Signal Processing*, vol. 43, pp. 2714–2723, Nov. 1995.

[12] G. Xu, H. Liu, L. Tong, and T. Kailath, "A least-squares approach to blind channel identification," *IEEE Trans. on Signal Processing*, vol. 43, pp. 2982–2993, Dec. 1995.

[13] H. C. Andrews and B. R. Hunt, *Digital Image Restoration*. Englewood Cliffs, NJ: Prentice Hall, 1977.

[14] H. J. Trussell and B. R. Hunt, "Improved methods of maximum *à posteriori* restoration," *IEEE Trans. on Computers*, vol. 27, pp. 57–62, Jan. 1979.

[15] A. M. Tekalp and G. Pavlović, "Restoration of scanned photographic images," in *Digital Image Restoration* (A. K. Katasaggelos, ed.), Berlin: Springer-Verlag, 1991.

[16] D. T. Kuan, A. A. Sawchuk, T. C. Strand, and P. Chavel, "Adaptive noise smoothing filter for images with signal-dependent noise," *IEEE Trans. on Pattern Analysis and Machine Intelligence*, vol. 7, pp. 165–177, Mar. 1985.

[17] C. R. Moloney and M. E. Jernigan, "Adaptive image estimation based on multiplicative superposition," *Optical Engineering*, vol. 29, pp. 478–487, May 1990.

[18] R. W. Schafer, R. M. Mersereau, and M. A. Richards, "Constrained iterative restoration algorithms," *Proc. of the IEEE*, vol. 69, pp. 432–450, Apr. 1981.

[19] A. P. Dempster, N. M. Laird, and D. B. Rubin, "Maximum likehood from incomplete data via the EM algorithm," *J. Roy. Stat. Soc., Ser. B*, vol. 39, pp. 1–38, Spring 1977.

[20] S. J. Reeves and R. M. Mersereau, "Blur identification by the method of generalized cross-validation," *IEEE Trans. on Image Processing*, vol. 1, pp. 301–311, July 1992.

[21] D. T. M. Slock and C. B. Papadias, "Further results on blind identification and equalization of multiple FIR channels," in *Proc. IEEE Int. Conf. Acoust., Speech, and Signal Processing*, vol. 3, (Detroit, MI), pp. 1964–1967, May 1995.

[22] T. K. Moon, "The Expectation-Maximization algorithm," *IEEE Signal Processing Magazine*, vol. 13, pp. 47–60, Nov. 1996.

[23] G. R. Ayers and J. C. Dainty, "Iterative blind deconvolution method and its applications," *Optics Letters*, vol. 13, pp. 547–549, July 1988.

[24] B. C. McCallum, "Blind deconvolution by simulated annealing," *Optics Communications*, vol. 75, pp. 101–105, Feb. 1990.

[25] D. Kundur and D. Hatzinakos, "Blind image restoration via recursive filtering using deterministic constraints," in *Proc. IEEE Int. Conf. Acoust., Speech, and Signal Processing*, vol. 4, (Atlanta, GA), pp. 2283–2286, May 1996.

[26] G. B. Giannakis and S. Halford, "Blind fractionally-spaced equalization of noisy FIR channels: Adaptive and optimal solutions," in *Proc. IEEE Int. Conf. Acoust., Speech, and Signal Processing*, vol. 3, (Detroit, MI), pp. 1972–1975, May 1995.

[27] G. D. Forney, Jr., "Minimal bases of rational vector spaces, with applications to multivariable linear systems," *SIAM Journal on Control*, vol. 13, pp. 493–520, May 1975.

[28] R. R. Bitmead, S. Y. Kung, B. D. O. Anderson, and T. Kailath, "Greatest common divisors via generalized Sylvester and Bezout matrices," *IEEE Trans. on Automatic Control*, vol. 23, pp. 1043–1047, Dec. 1978.

[29] L. Tong, G. Xu, B. Hassibi, and T. Kailath, "Blind channel identification based on second-order statistics: A frequency-domain approach," *IEEE Trans. on Information Theory*, vol. 41, pp. 329–334, Jan. 1995.

List of Figures

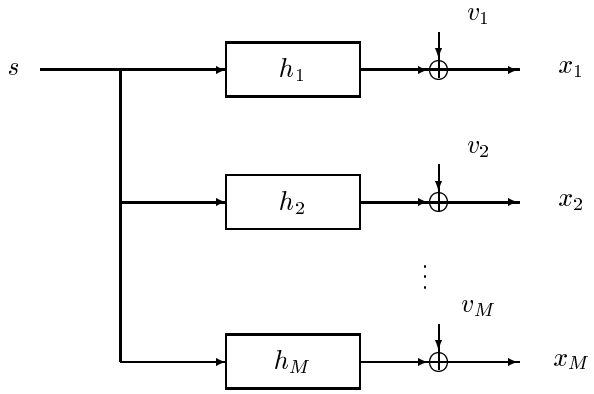

Figure 1: Single-input multiple-output image-blur model.

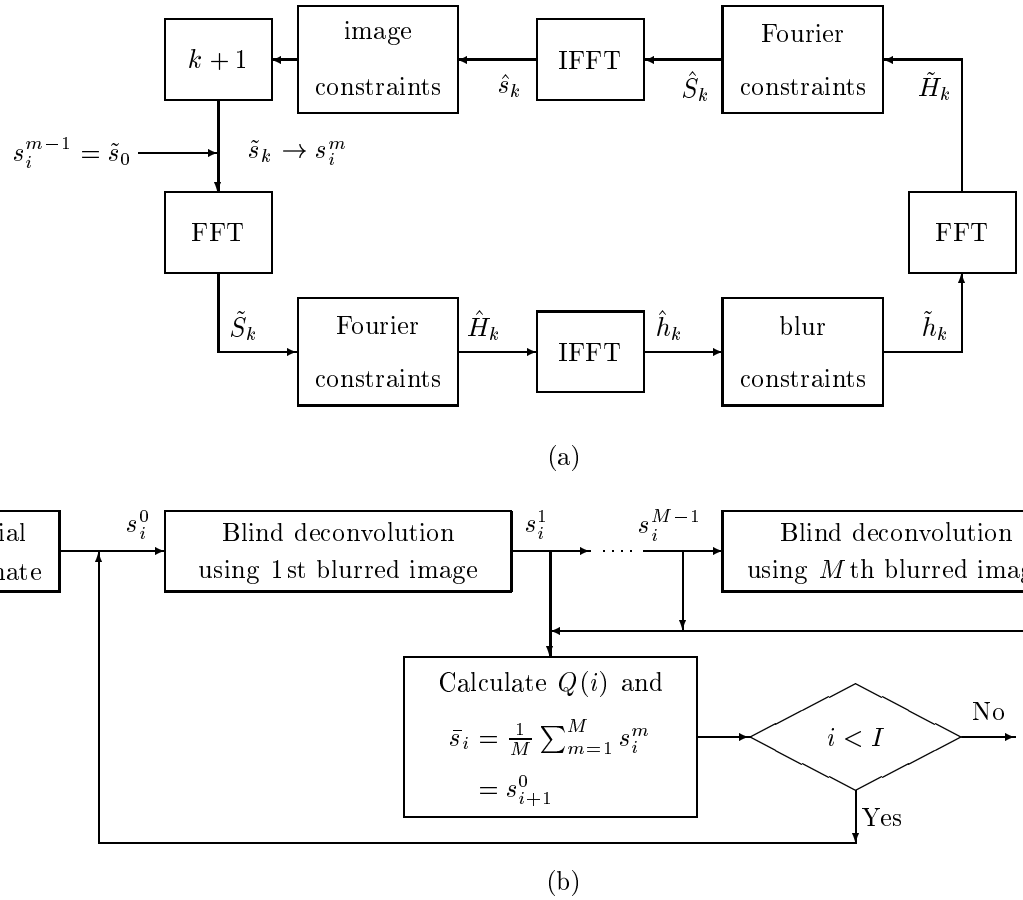

Figure 2: Flow charts of (a) the iterative single-channel blind image restoration algorithm and (b) the iterative multichannel blind image restoration algorithm.

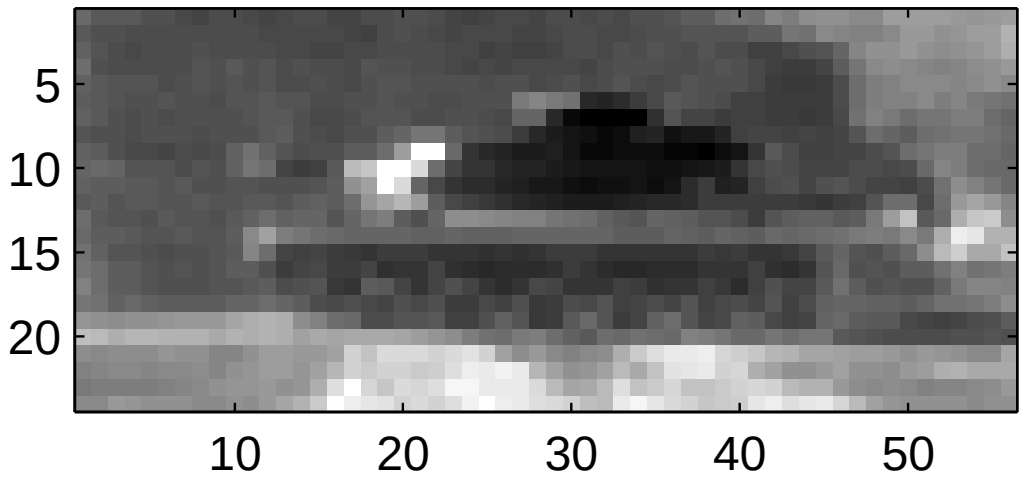

Figure 3: Original tank image.

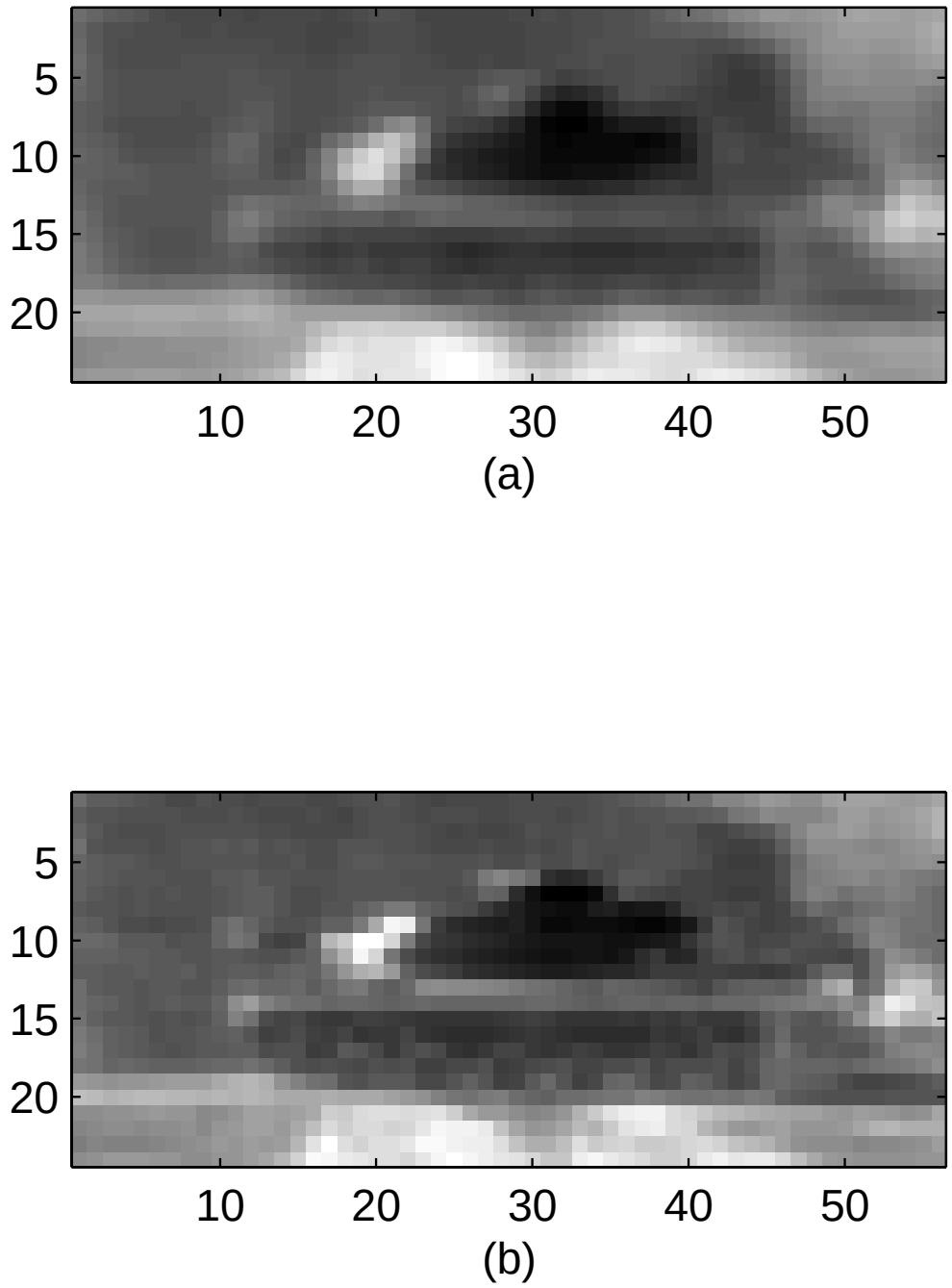

Figure 4: 3×3 blur functions, 3 channels, and $SNR = 60$ dB : (a) one of the blurred images, and (b) the restored image.

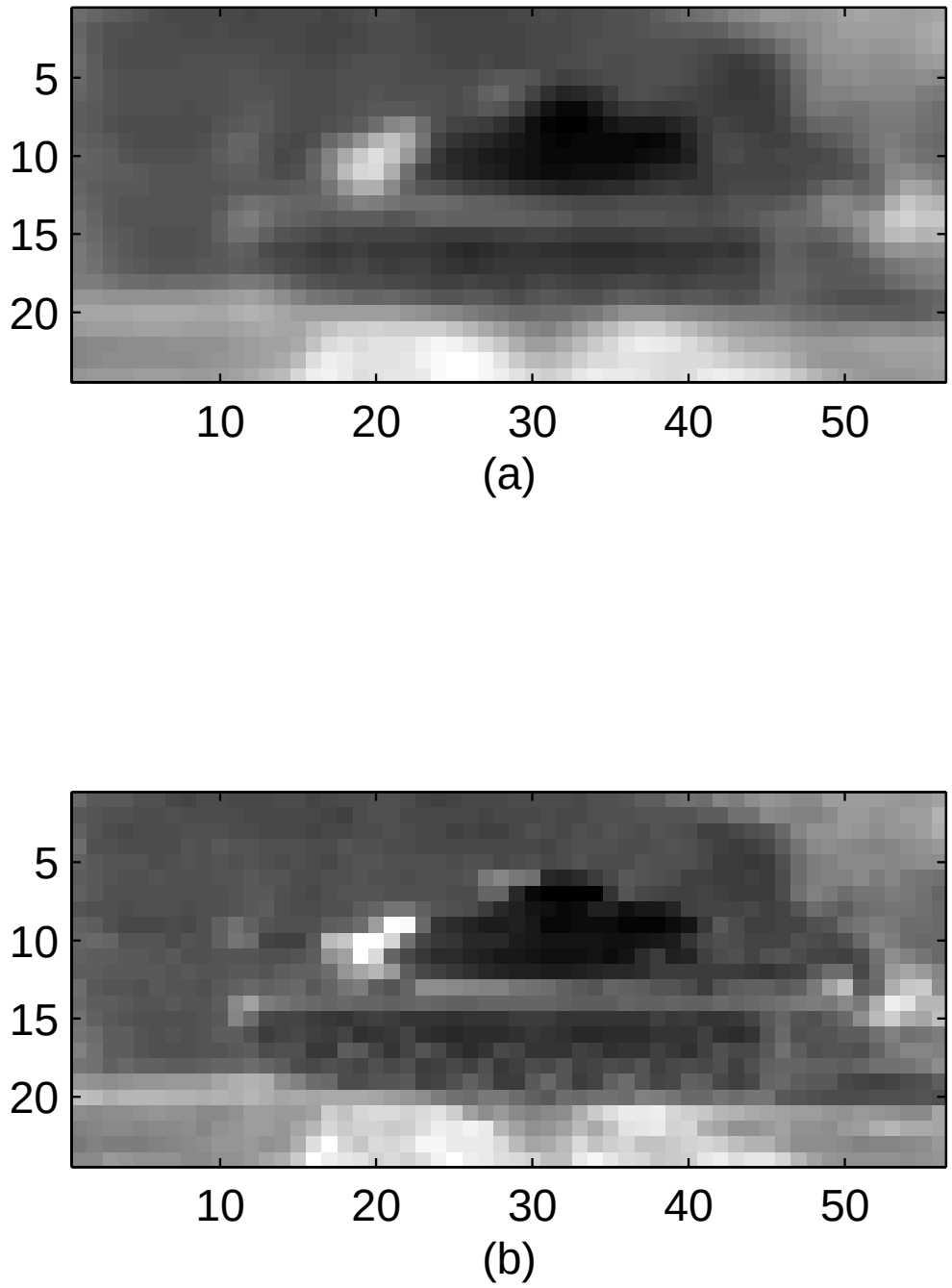

Figure 5: 3×3 blur functions, 6 channels, and $SNR = 60$ dB : (a) one of the blurred images, and (b) the restored image.

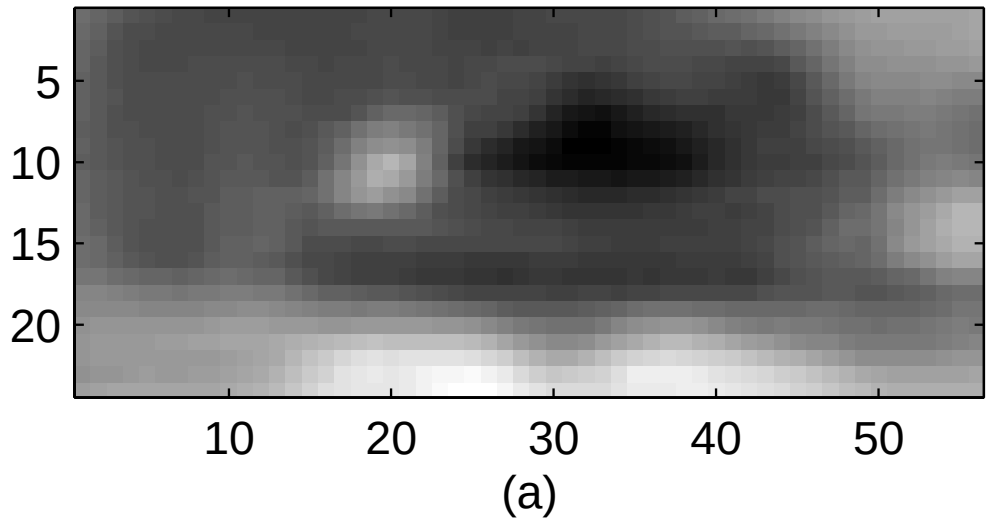

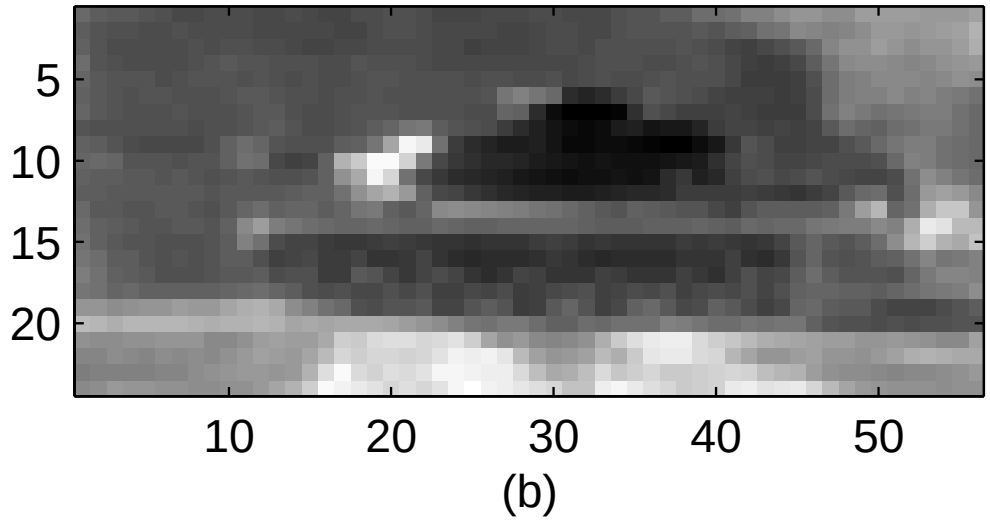

Figure 6: 5×5 blur functions, 6 channels, and $SNR = 60$ dB : (a) one of the blurred images, and (b) the restored image.

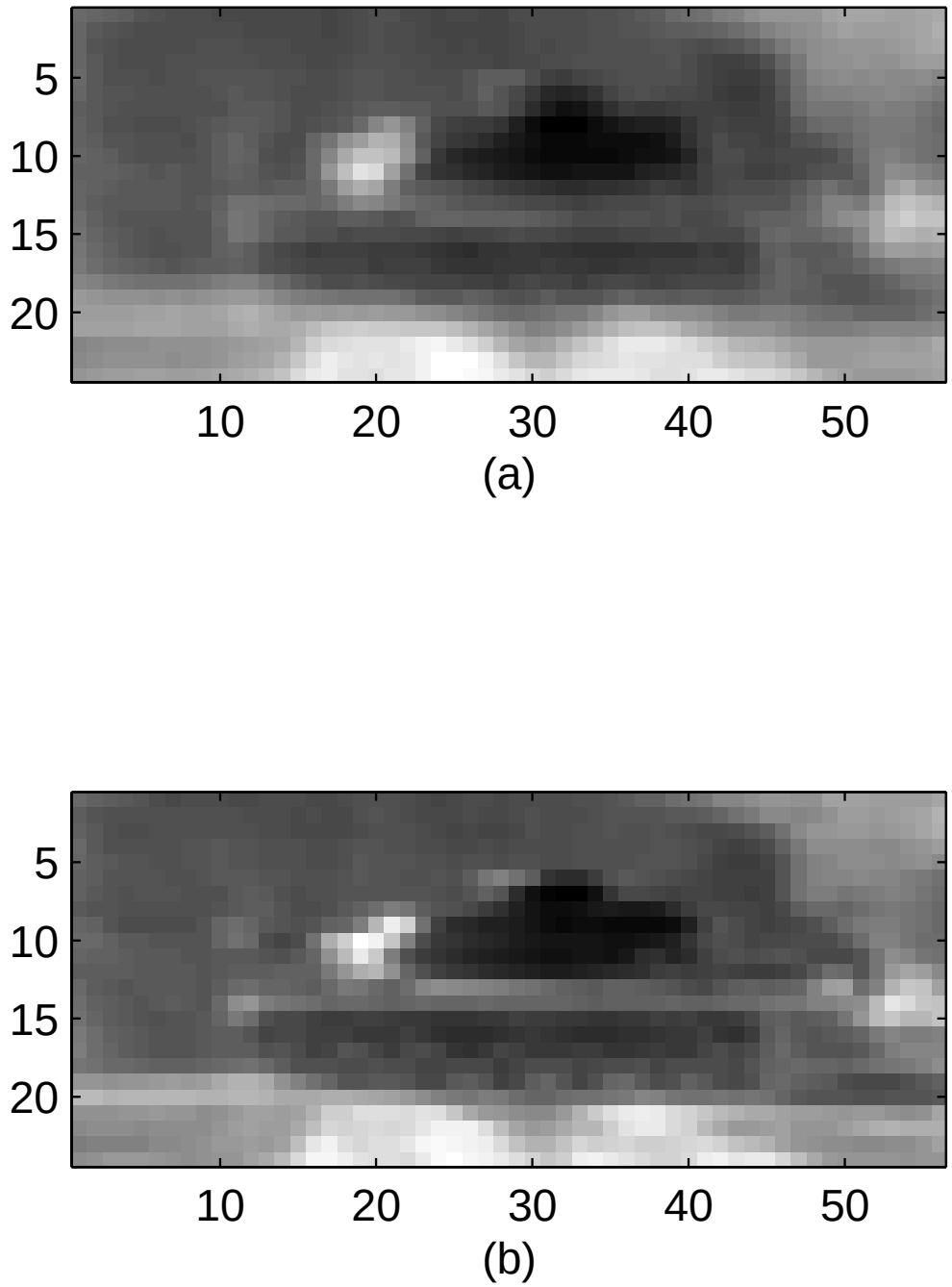

Figure 7: 3×3 blur functions, 3 channels, and $SNR = 50$ dB : (a) one of the blurred images, and (b) the restored image.

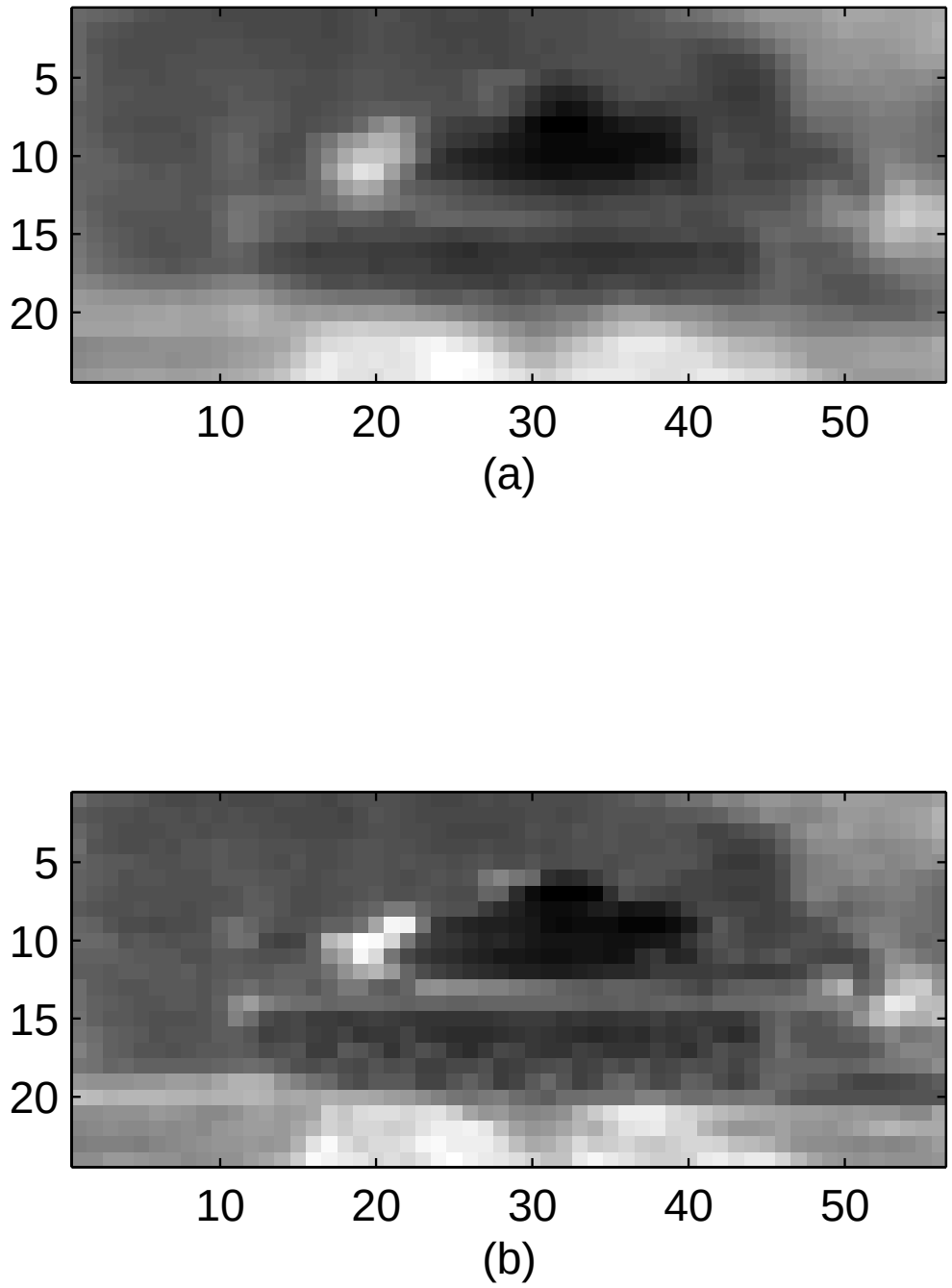

Figure 8: 3×3 blur functions, 6 channels, and $SNR = 50$ dB : (a) one of the blurred images, and (b) the restored image.

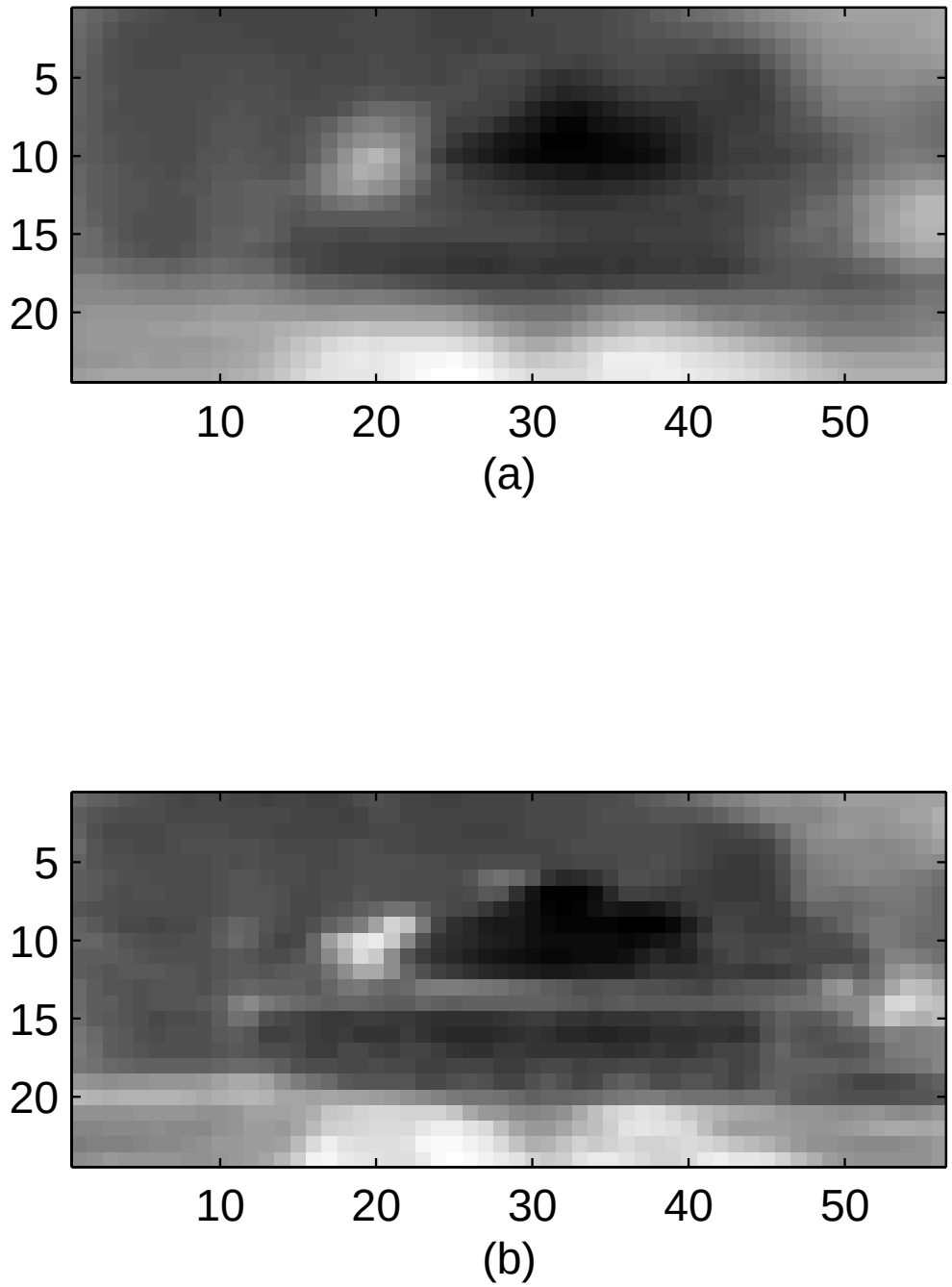

Figure 9: 5×5 blur functions, 6 channels, and $SNR = 50$ dB : (a) one of the blurred images, and (b) the restored image.